Vector correlations and alignment parameters in the photodissociation of HF and DF

G. G. Balint-Kurti and A. J. Orr-Ewing
School of Chemistry, University of Bristol, Bristol BS8 1TS, United Kingdom

J. A. Beswick
Laboratoire de Collisions, Agrégats et Réactivité, IRSAMC, Université Paul Sabatier, 31062 Toulouse, France

Alex Brown
Department of Physics and Astronomy, University of Alabama, Tuscaloosa, Alabama 35487-0324

O. S. Vasyutinskii
Ioffe Physico-Technical Institute, Russian Academy of Sciences, 194021 St.-Petersburg, Russia

(Received 5 February 2002; accepted 19 March 2002)

Orientation and alignment parameters have been computed from first principles for the photodissociation of the HF and DF diatomic molecules. The calculations are entirely *ab initio* and the break-up dynamics of the molecule is treated rigorously taking account of the electronically nonadiabatic dynamics on three coupled adiabatic electronic potential energy curves. The potential energy curves and spin–orbit interactions, which have been previously reported [J. Chem. Phys. **113**, 1870 (2000)], are computed using *ab initio* molecular electronic structure computer codes. These are then used to compute photofragmentation **T** matrix elements using a time-dependent quantum mechanical wave packet treatment and from these a complete set of anisotropy parameters with rank up to $K=3$ is computed. The predicted vector correlations and alignment parameters are presented as a function of energy for HF and DF initially in both their ground and first excited vibrational states. The parameters predicted for the molecules which are initially in their excited vibrational states display a pronounced sharp energy dependence arising from the nodal structure of the initial vibrational wavefunction. The theoretical results are analyzed using a simple model of the dynamics and it is demonstrated how the magnitude and relative phases of the photofragmentation **T** matrix elements can be deduced from the experimentally measured alignment parameters. No experimental measurements have yet been made of alignment parameters for hydrogen halide diatomics and the present results provide the first predictions of these quantities which may be compared with future experimental observations. © *2002 American Institute of Physics.*
[DOI: 10.1063/1.1476937]

I. INTRODUCTION

It is one of the central aims of science to understand, in as much detail as possible, the elementary molecular processes which occur in nature. The absorption of ultraviolet light by a molecule and its subsequent photodissociation is an important example of such a process and is one we seek to understand better in the present work. Data obtained from the examination of the products of a photodissociation process constitute a rich source of potential information about the electronic structure of a molecule and of its excited electronic states. The role of theory is to model the entire photofragmentation process as accurately as possible and through this to learn about both the electronic structure of the molecule and about the detailed dynamics of the breakup process.

Advances in laser technology and in the techniques used to detect and examine the atomic and molecular fragments of photodissociation processes have totally revolutionalized the amount and detailed level of information which can now be derived from a photofragmentation experiment.[1–6] In parallel with these experimental advances, there have been advances in theoretical methods used to describe and analyze the observations, mainly at a phenomenological level.[7–12] Light is intrinsically polarized. The use of laser light to photodissociate a molecule is therefore inevitably associated with some directional preference that is reflected in the distribution of the products. The theory of orientation and alignment effects has systematized the analysis of the experimental results and these can now be analyzed to yield a set of irreducible parameters that uniquely characterize correlation of the different vector quantities that can be associated with the photofragments.

Despite all the advances in the theory, prior to the present paper, there has been no *ab initio* prediction of any molecular orientation and alignment parameters for a molecular photodissociation process. We present the first such calculations in this paper. (See, however, Ref. 13 where *ab initio* potential curves are used coupled with an approximate treatment of the photodissociation dynamics.) The potential

energy curves for the lowest four electronic states of the HF molecule, the associated transition dipole moment matrix elements, and the spin–orbit coupling curves have been computed previously[14] using *ab initio* electronic structure theory and have been utilized to make predictions of scalar properties, i.e., total cross-section and branching fractions, for the photofragmentation process. In the present work, these molecular quantities are employed within the context of a time-dependent quantum mechanical wave packet treatment to compute photofragmentation **T** matrix elements. This wave packet treatment takes full account of the electronically nonadiabatic transitions which occur during the breakup of the molecule. The photofragmentation **T** matrix elements contain all possible information about the photofragmentation process. They enable us, through the use of the well-established theoretical framework of vector correlation parameters,[12] to predict the associated irreducible orientation and alignment parameters.

The paper is organized in the following manner: Section II briefly reviews the theory. This section is supported by an appendix, which tabulates the detailed form of all of the orientation and alignment parameters. The appendix also gives the relationships, for the particular case under discussion in this paper, of the two different forms of the orientation and alignment parameters which are most widely used. Section III describes the methods used in the current calculations and Sec. IV presents our results for the HF molecule. A short summary is given in Sec. V.

II. THEORY: GENERAL EXPRESSION FOR PHOTOFRAGMENT STATE MULTIPOLES AND ANISOTROPY PARAMETERS

Let us consider the photodissociation of a molecule AB to produce fragments A and B. The fragments A and B have angular momenta $\mathbf{j_A}$ and $\mathbf{j_B}$, respectively, and these have z components of m_A and m_B about the space fixed $\mathbf{Z}$ axis. The initial and the final total angular momenta of the molecule are $\mathbf{J_i}$ and $\mathbf{J}$, respectively, and the corresponding space-fixed z components are M_i and M.

If the interaction of radiation with the molecule is treated using the dipole approximation, and if first order time-dependent perturbation theory is used, the generalized photofragmentation cross section $\sigma(\hat{\mathbf{k}}E,\tilde{n},\tilde{n}')$ can be written as[15–17]

$$\sigma(\hat{\mathbf{k}}E,\tilde{n}',\tilde{n}) = \frac{2\pi^2\nu}{c\epsilon_0(2J_i+1)} \times \sum_{M_i} \langle \Psi^{-(\hat{\mathbf{k}}\tilde{n}')}(\mathbf{R},\mathbf{r},E)|\hat{\mathbf{d}}\cdot\mathbf{e}|\Psi_{J_iM_i}\rangle \times \langle \Psi^{-(\hat{\mathbf{k}}\tilde{n})}(\mathbf{R},\mathbf{r},E)|\hat{\mathbf{d}}\cdot\mathbf{e}|\Psi_{J_iM_i}\rangle^*, \quad (1)$$

where ν is the frequency of the incident light, $\mathbf{e}$ is a polarization vector, $\hat{\mathbf{d}}$ is a dipole operator, $\mathbf{R}$ is the vector connecting the centers of mass of the fragments, while $\mathbf{r}$ denotes collectively all the internal coordinates of fragments. $\Psi_{J_iM_i}$ is the wave function of the initial molecular state and $\Psi^{-(\hat{\mathbf{k}}\tilde{n})}(\mathbf{R},\mathbf{r},E)$ is the dissociative wave function describing two photofragments flying apart with total energy E *in a direction specified by the unit vector* $\hat{\mathbf{k}}$ *with polar angles* θ, ϕ. The index $\tilde{n}$ is the set of quantum numbers specifying the electronic states and angular momenta (j_A,m_A,j_B,m_B) of the fragments.

The generalized differential cross section $\sigma(\hat{\mathbf{k}}E,\tilde{n}',\tilde{n})$ in Eq. (1) relates to the case of an isotropic distribution of the angular momenta of the parent molecule. Its diagonal elements are the normal photofragmentation cross sections. The off-diagonal elements are the vector correlation coefficients which have been the subject of many recent important theoretical and experimental investigations.[7,8,18] For instance, if $\tilde{n}\equiv j_A,m_A,j_B,m_B$, the cross section matrix elements $\sigma(\hat{\mathbf{k}}E,\tilde{n}',\tilde{n})$ give the probability of fragments flying apart in a direction specified by the polar angles θ, ϕ. The diagonal elements of the matrix $(\tilde{n}'=\tilde{n})$ give the probability of producing the fragments with a specific value of the fragment angular momenta and of their space fixed z components, while the off-diagonal elements $(\tilde{n}'\neq\tilde{n})$ describe the coherence between states with different values of these quantum numbers.[19]

The experiments usually involve the detection of only one of the two fragments and therefore do not yield simultaneous information concerning both of the fragments. The cross section corresponding to such an experiment involves averaging over the quantum numbers of the other, nondetected, fragment. This averaging is performed by taking the trace of the generalized cross section over the quantum numbers that are not actually measured, i.e.,

$$\sigma^{j_A}_{m_A';m_A}(\theta,\phi) = \sum_{j_Bm_B} \sigma(\hat{\mathbf{k}}E;j_A,m_A',j_B,m_B;j_A,m_A,j_B,m_B). \quad (2)$$

It is convenient to express the elements of the generalized differential cross section [Eq. (2)] $\sigma^{j_A}_{m_A';m_A}(\theta,\phi)$ in terms of the angular momentum state multipoles $\rho^{(j_A)}_{KQ}(\theta,\phi)$, which are dimensionless spherical tensors of rank K and projection Q.[19–21] If the total cross section σ_0 is chosen as a normalization factor, the corresponding laboratory frame state multipole can be written as

$$\rho^{(j_A)}_{KQ}(\theta,\phi) = \frac{1}{(2j_A+1)^{1/2}\sigma_0} \sum_{m_A',m_A} (-1)^{j_A-m_A}(2K+1)^{1/2} \times \begin{pmatrix} j_A & j_A & K \\ m_A & -m_A' & -Q \end{pmatrix} \sigma^{j_A}_{m_A';m_A}(\theta,\phi), \quad (3)$$

where $\sigma_0=(2j_A+1)^{-1/2}\langle \mathrm{Tr}[\sigma^{j_A}_{m_A';m_A}(\theta,\phi)]\rangle$ and the angle brackets signify integration over the angles θ and ϕ. The factor in the parentheses in Eq. (3) is a $3-j$ symbol while the prefactor $(2j_A+1)^{-1/2}$ is used to fulfill the normalization condition $\langle \rho^{(j_A)}_{00}(\theta,\phi)\rangle=(2j_A+1)^{-1/2}$.[19] The expression for the fragment state multipole $\rho^{(j_A)}_{KQ}(\theta,\phi)$ for the case $j_B=0$ has recently been studied in Ref. 18. In subsequent expressions, the superscript (j_A) will be dropped for convenience.

Ab initio molecular electronic structure calculations are performed in the molecular frame, in which the unique or z

axis is fixed in the molecule. In the case of a diatomic molecule this is the molecular axis. The most accurate calculations, of the type considered in the present work, include both the orbital and spin angular momenta of the electrons. The total angular momentum of fragment A is denoted by j_A and its component about the molecular axis is denoted by Ω_A. A similar notation is used for the angular momenta of fragment B. In the presence of spin–orbit interaction the only good quantum number, for a nonrotating molecule, is the component of the total angular momentum about the molecular axis, $\Omega=\Omega_A+\Omega_B$. The expansion of the total electronic wave function, $\Psi^{\rm el}$, in terms of the "spin–orbit coupled" basis, $|j_A\Omega_A\rangle|j_B\Omega_B\rangle$ may be written in the form

$$\Psi^{\rm el}_{n,\Omega} \overset{R\to\infty}{\to} \sum_{\Omega_A,\Omega_B} \mathcal{T}^{n\Omega}_{j_A\Omega_A j_B\Omega_B} \hat{A}|j_A\Omega_A\rangle|j_B\Omega_B\rangle, \tag{4}$$

where $\hat{A}$ is an antisymmetrization operator (see, e.g., Ref. 22) and the index n differentiates between different adiabatic electronic states with the same value of Ω.

The matrices $\mathcal{T}^{n\Omega}_{j_A\Omega_A j_B\Omega_B}$ in Eq. (4) are the expansion coefficients of the adiabatic molecular electronic states in terms of the fragment basis ($|j_A\Omega_A\rangle|j_B\Omega_B\rangle$) in the asymptotic region $R\to\infty$. In general these matrices *are not* the Clebsch–Gordan coefficients, they depend on the nature of the long-range interaction between the fragments and can be determined by diagonalizing the Hamiltonian matrix expressed in the fragment basis in the asymptotic region.[23–25]

Using Eqs. (1), (3), (4) and applying the properties of the $3-j$ symbols and Wigner matrices in a way analogous to that used in Ref. 18, the fragment A state multipole, Eq. (3), in the axial recoil approximation can be written as (see Appendix A):

$$\begin{aligned}\rho_{KQ}(\theta,\phi)=&\frac{3}{4\pi}\left(\frac{2K+1}{2j_A+1}\right)^{1/2}\sum_{k_d,q_d,Q'}\sum_{q,q'}(-1)^{K+q'}\\&\times E_{k_dq_d}(\mathbf{e})\frac{f_K(q,q')}{f_0(0,0)+2f_0(1,1)}(2k_d+1)^{1/2}\\&\times\begin{pmatrix}1&1&k_d\\q'&-q&-Q'\end{pmatrix}D^{K*}_{QQ'}(\phi,\theta,0)\\&\times D^{k_d}_{q_dQ'}(\phi,\theta,0),\end{aligned} \tag{5}$$

where $D^K_{QQ'}(\phi,\theta,0)$ are Wigner rotation matrix elements,[26] $Q'=q'-q$ is a component of the rank K state multipole in the molecular frame, and $E_{k_dq_d}(\mathbf{e})$ are elements of the dissociation light polarization matrix.[20,21,27] The molecular-frame component Q' can only take the values $Q'=-2,-1,0,1,2$.[18]

The axial recoil approximation is valid in the limit of a fast dissociation process. In this approximation the body-fixed projection of the total angular momentum on the molecular axis (Ω) is treated as a good quantum number and the overall rotation of the molecule is neglected.

The expression for the state multipoles of fragment B can be obtained from Eq. (5) by exchanging subscripts A and B. In general the multipole rank, K, in Eq. (5) ranges from $K=0$ to $K=2j_A$.[19,20] The description of the hydrogen atom fragment ($j_A=\frac{1}{2}$) arising from the photolysis therefore requires only state multipoles of rank $K=0$ (population) and rank $K=1$ (orientation). For the fluorine fragment ($j_B=\frac{1}{2},\frac{3}{2}$) the complete set of state multipoles contains $K=0$, $K=1$ and also $K=2$ (alignment) and $K=3$ (octupole moment). For each state multipole, the angular dependence in Eq. (5) is universal and does not depend on the dissociation dynamics of a particular molecule. The angular dependencies of the state multipoles with the ranks $K=0,1,2$ and with all possible projections, $Q=-K\ldots K$, have been presented for several different experimental arrangements or geometries in Refs. 11 and 12. The individual state multipoles can, in principle, be observed experimentally using, for instance, ion imaging techniques,[1,2,11,28] or by measurement of Doppler or time-of-flight peak profiles.[3,5]

In the above description we have neglected fragment nuclear spins. This is justified as the duration of the dissociation process is typically much smaller than the Heisenberg uncertainty time, $\delta t=\hbar/(2\,\delta E)$ associated with the hyperfine splitting in the atoms. Therefore, the nuclear spins do not affect the dynamics of the photodissociation process. However, the hyperfine interaction in the final fragments is important and results in partial depolarization of the fragment electron angular momenta.[20]

The quantities $f_K(q,q')$ in Eq. (5) are *dynamical functions*. The indices q,q' are the vector spherical harmonic components[20,29] of the molecular electric dipole moment with respect to the recoil axis. They can take only the values 0 or ±1, corresponding to parallel or perpendicular electronic transitions, respectively. The dynamical functions in Eq. (2) are defined as

$$\begin{aligned}f_K(q,q')=&\sum_{n,\Omega,\Omega_A,n',\Omega',\Omega'_A}(-1)^{K+j_A+\Omega'_A}\\&\times\begin{pmatrix}j_A&j_A&K\\-\Omega_A&\Omega'_A&q-q'\end{pmatrix}\\&\times\mathcal{T}^{n\Omega}_{j_A\Omega_A j_B\Omega_B}(\mathcal{T}^{n'\Omega'}_{j_A\Omega'_A j_B\Omega_B})^*\\&\times\langle\Psi^-_{n,\Omega}(R,\mathbf{r},E)|\hat{\mathbf{d}}_q|\Psi_{\Omega_i}\rangle^*\\&\times\langle\Psi^-_{n',\Omega'}(R,\mathbf{r},E)|\hat{\mathbf{d}}_{q'}|\Psi_{\Omega_i}\rangle,\end{aligned} \tag{6}$$

where $\Psi^-_{n,\Omega}(R,\mathbf{r},E)$ is the scattering wave function for the channel n,Ω in the body-fixed coordinate system[14,15,38] and the initial and final z components of the total electronic angular momentum about the molecular axis are related by $\Omega=\Omega_i+q$. The matrix elements $\langle\Psi^-_{n,\Omega}(R,\mathbf{r},E)|\hat{\mathbf{d}}_q|\Psi_{\Omega_i}\rangle$ are the photofragmentation $\mathbf{T}$ matrix elements.[15,16] These $\mathbf{T}$ matrix elements are computed exactly using a time-dependent wave packet formalism[17] in the present work.

The summation in Eq. (6) is over all indices n, Ω, n', Ω', Ω_A, Ω'_A. No explicit summation over Ω_B is necessary as the relationship $\Omega=\Omega_A+\Omega_B$ ensures that this summation is effectively performed. Due to symmetry properties of the $3-j$ symbols, the following relation is fulfilled: $q-q'=\Omega_A-\Omega'_A=\Omega-\Omega'$. Therefore, the diagonal elements of the dynamical functions $f_K(q,q')$ in Eq. (6) with $q=q'$ cor-

respond to incoherent excitation of parallel, or perpendicular transitions, while the off-diagonal elements with $q \neq q'$ correspond to coherent excitation of different molecular continua. It should be noted that in the definition of the dynamical factors, Eq. (6), only Ω_B and j_B occur and no Ω_B' or j_B'. This is because we are taking the average or trace over these quantum numbers.

The dynamical functions obey the following symmetry relations:[24]

$$f_K(q,q') = (-1)^K f_K(-q,-q') = (-1)^{q-q'} f_K^*(q',q). \tag{7}$$

The functions, $f_K(q,q')$, contain all information about the transition dipole moments, phases, and other fragmentation dynamics of a particular molecule. The quantum mechanical observables which can be determined from experiment are the magnitude of the total cross section, σ_0, and the dimensionless *anisotropy parameters*. The anisotropy parameters are normalized combinations of the dynamical functions of rank K. The zeroth-rank anisotropy parameter is the well-known β parameter which can be expressed in terms of the dynamical functions as[18]

$$\beta = \frac{2[f_0(0,0) - f_0(1,1)]}{2 f_0(1,1) + f_0(0,0)}. \tag{8}$$

Two alternative sets of anisotropy parameters have recently been introduced for rank $K>0$. One of these sets, α_K, γ_K, η_K, s_K, and η_K,[30] is related to the *laboratory frame* orientation and alignment of the photofragment angular momenta. The spatial modulations in an ion image, Doppler profile, or time of flight mass spectroscopy (TOFMS) profile, that result from orientation and alignment effects in the photofragmentation process, often constitute a relatively small fraction of the total signal. A powerful experimental procedure for separating the orientation and alignment contribution from the population term $\rho_{00}(\theta,\phi)$, and also from the angular distribution of the photofragments associated with the zero rank anisotropy parameter β, has recently been developed.[12] The other set of orientation and alignment parameters, $\mathbf{a}_{\tilde{Q}}^{(K)}(p)$, where $\tilde{Q} = -Q$ and $p = \perp$, $\parallel$, or $(\perp, \parallel)$ corresponding to pure perpendicular, pure parallel, or mixed perpendicular/parallel excitation, is related to the *molecular frame* orientation and alignment of the photofragment angular momenta.[9,10,31] This set of parameters is more suitable for a theoretical analysis and is therefore used here. The parameters of both the sets which are relevant to this study are defined in terms of the dynamical functions and are related to each other in Appendix B.

III. DETERMINATION OF THE DYNAMICAL FUNCTIONS

The equation for the dynamical functions, Eq. (6), involves a sum of products of the $3-j$ symbols, the expansion coefficients of the adiabatic electronic molecular wave functions at large separations in terms of the wave functions of the separate atoms ($\mathcal{T}^{n\Omega}_{j_A\Omega_A j_B\Omega_B}$), and the photofragmentation **T** matrix elements, $\langle \Psi^-_{n,\Omega} | \hat{\mathbf{d}}_q | \Psi_{\Omega_i} \rangle$. In the case of HF, photodissociation takes place via the three lowest $\Omega = 1$ excited electronic states and the quantum numbers K and q,q' in Eq. (6) are restricted to the values $K = 0,1,2,3$ and $q,q' = \pm 1$.

A. Photofragmentation T matrix elements

The initial step in the calculation of the photofragmentation **T** matrix elements using a time-dependent wave packet formalism is the setting up of an initial wave packet. This wave packet may be written as

$$\phi_n(\mathbf{R}, t=0) = \mathbf{d}^n_{q'}(\mathbf{R}) \Psi_{\Omega_i}(\mathbf{R}), \tag{9}$$

where $\phi_n(\mathbf{R}, t=0)$ represents an initial wave packet on the nth electronically adiabatic potential energy surface and $\mathbf{d}^n_{q'}(\mathbf{R})$ is the transition dipole moment for excitation from the initial electronic state.[29,32,33]

Following the setting up of the initial wave packets, they are propagated forward in time by solving the time-dependent Schrödinger equation. This requires the simultaneous solution of coupled time-dependent equations. The results are analyzed by taking cuts through the wave packets at each time step at a fixed, large value of the scattering coordinate, $R = R_\infty$. If we specialize the treatment now to the case of a diatomic molecule, so that we can replace **R** by R, then we can write the energy dependent coefficients obtained by taking the Fourier transform over time of the cuts through the time-dependent wave packets as (see Ref. 14):

$$A_n(R_\infty, E) = \frac{1}{2\pi} \int_0^\infty \phi_n(R_\infty, t) \exp[i(E_i + h\nu)t/\hbar] dt. \tag{10}$$

The analysis of Ref. 32 shows that these energy dependent coefficients are related to the photofragmentation **T** matrix elements by the relationship:

$$\langle \Psi^-_{n,\Omega}(R, \mathbf{r}, E) | \hat{\mathbf{d}}_q | \Psi_{\Omega_i} \rangle = i \left(\frac{h^2 k_v}{2\pi\mu} \right)^{1/2} \exp(-ik_v R_\infty) A_n(R_\infty, E), \tag{11}$$

where the matrix element on the left hand side of the above equation is the photofragmentation **T** matrix element associated with the asymptotic channel n, k_v is the asymptotic wave vector for this channel and μ is the reduced mass of the two photofragments.

B. Adiabatic electronic wave functions at large separations

The low lying energy states of the HF molecule correlate adiabatically at large internuclear distance with two spin–orbit energy levels corresponding to the $H(^2S_{1/2}) + F(^2P_{3/2})$ and $H(^2S_{1/2}) + F(^2P_{1/2})$ pairs of fragments. In the molecular region these states split into 12 substates (four of them being degenerate): there is one $|\Omega| = 2$ level (two substates), three $|\Omega| = 1$ levels (six substates), two $\Omega = 0^+$ substates, and two $\Omega = 0^-$ substates. The major contribution to the long-range interaction for both levels is the van der Waals interaction resulting in a $-C/R^6$ energy dependence, where C is a constant. The corresponding long-range energy states and molecular wave functions determined by using second order perturbation theory[34] are presented in Table I. According to

TABLE I. Energy levels and molecular wave functions for van der Waals interatomic interaction.

Energy of the molecular state	Molecular state $\lvert n,\Omega^{\sigma}\rangle$	Expansion of the wave function $\lvert n,\Omega^{\sigma}\rangle$ over the atomic states $\lvert j_A\Omega_A;j_B\Omega_B\rangle$
$\Delta_{so}-\frac{1}{\sqrt{3}R^6}\epsilon(0,0)$	$\lvert\beta,0^+\rangle$	$\frac{1}{\sqrt{2}}\left(\left\lvert\frac{1}{2}\frac{1}{2};\frac{1}{2}-\frac{1}{2}\right\rangle+\left\lvert\frac{1}{2}-\frac{1}{2};\frac{1}{2}\frac{1}{2}\right\rangle\right)$
	$\lvert\beta,0^-\rangle$	$\frac{1}{\sqrt{2}}\left(\left\lvert\frac{1}{2}\frac{1}{2};\frac{1}{2}-\frac{1}{2}\right\rangle-\left\lvert\frac{1}{2}-\frac{1}{2};\frac{1}{2}\frac{1}{2}\right\rangle\right)$
	$\lvert\gamma,1\rangle$	$\left\lvert\frac{1}{2}\frac{1}{2};\frac{1}{2}\frac{1}{2}\right\rangle$
$-\frac{1}{\sqrt{3}R^6}\left[\epsilon(0,0)-\frac{\epsilon(0,2)}{2\sqrt{5}}\right]$	$\lvert 2\rangle$	$\left\lvert\frac{1}{2}\frac{1}{2};\frac{3}{2}\frac{3}{2}\right\rangle$
	$\lvert\beta,1\rangle$	$\left\lvert\frac{1}{2}-\frac{1}{2};\frac{3}{2}\frac{3}{2}\right\rangle$
$-\frac{1}{\sqrt{3}R^6}\left[\epsilon(0,0)+\frac{\epsilon(0,2)}{2\sqrt{5}}\right]$	$\lvert\alpha,0^+\rangle$	$\frac{1}{\sqrt{2}}\left(\left\lvert\frac{1}{2}\frac{1}{2};\frac{3}{2}-\frac{1}{2}\right\rangle-\left\lvert\frac{1}{2}-\frac{1}{2};\frac{3}{2}\frac{1}{2}\right\rangle\right)$
	$\lvert\alpha,0^-\rangle$	$\frac{1}{\sqrt{2}}\left(\left\lvert\frac{1}{2}\frac{1}{2};\frac{3}{2}-\frac{1}{2}\right\rangle+\left\lvert\frac{1}{2}-\frac{1}{2};\frac{3}{2}\frac{1}{2}\right\rangle\right)$
	$\lvert\alpha,1\rangle$	$\left\lvert\frac{1}{2}\frac{1}{2};\frac{3}{2}\frac{1}{2}\right\rangle$

the Hund's case *c* classification we denote the molecular wave functions in Table I as $|n,\Omega^{\sigma}\rangle$, where $\sigma=\pm$ is a reflection character for the $\Omega=0$ energy substates and $n=\alpha$, β, or γ is an index labeling the different substates with the same $|\Omega|$ quantum number in order of increasing energy. As the ground electronic state of HF has $\Omega=0^+$, and the only nonzero transition dipole moment is to an electronic state with $\Omega=1$, only the excited energy states $|\alpha,1\rangle$, $|\beta,1\rangle$, and $|\gamma,1\rangle$ are involved in the photodissociation dynamics.[14] At smaller internuclear distances these states correlate adiabatically with the $a\,^3\Pi_1$, $A\,^1\Pi_1$, and $1\,^3\Sigma_1^+$ molecular energy states, respectively. Only the second of these states can be optically excited from the molecular ground $X\,^1\Sigma_0^+$ state.[14] The $\mathcal{T}^{n\Omega}_{j_A\Omega_A j_B\Omega_B}$ matrix elements are the expansion coefficients in the third column in Table I.

The value Δ_{so} in the first column of Table I is a spin–orbit energy splitting in the fluorine atom and the values $\epsilon(0,0)$ and $\epsilon(0,2)$ are defined as[22]

$$\epsilon(\chi_H,\chi_F)=\frac{2}{\pi}\int_0^{\infty}d\omega\langle L_H||\alpha_{\chi_H}(\omega)||L_H\rangle \times\langle L_F||\alpha_{\chi_F}(\omega)||L_F\rangle, \tag{12}$$

where $\alpha_{\chi_H}(\omega)$ and $\alpha_{\chi_F}(\omega)$ are irreducible dipole dynamical polarizabilities of the $H(^2S)$ and $F(^2P)$ atoms, respectively. The values in the angular brackets in Eq. (12) are reduced matrix elements where $L_H=0$, $L_F=1$ are the corresponding atomic orbital angular momenta.

IV. RESULTS AND DISCUSSION

A. Anisotropy parameters arising from the photodissociation of HF($v=0$)

The potential energy curves and spin–orbit coupling matrix elements used for the HF and DF molecules were calculated using the MOLPRO *ab initio* electronic structure code[35] and have been reported in our previous paper (see Ref. 14). A large augmented correlation-consistent valence quintuple zeta (av5z) basis set of Dunning *et al.*[36] was used for the *ab initio* calculations. This consisted of a total of 146 contracted orbitals and included *g* functions on the hydrogen atom and *h* functions on the fluorine. These potential energy curves and spin–orbit coupling matrix elements were used, as described above, to compute the photofragmentation **T** matrix elements. The treatment of the electronically nonadiabatic dynamics, which allows the wave packet flux to pass from one adiabatic electronic state to another, has been fully described in a previous paper.[37]

Figure 1 shows snapshots of the wave packets in the three excited electronic states at four different times. The initial wave packet is almost entirely in the $A\,^1\Pi_1$ state. There is in fact a very small contribution to the initial wave packet in the $a\,^3\Pi_1$ state, but this contribution is too small to be visible on the graph. At 4.8 femtoseconds (fs) some of the wave packet amplitude has been transferred, through electronically nonadiabatic transitions to the $1\,^3\Sigma_1$ state. At 9.7 fs the amplitude of the wave packet in the $1\,^3\Sigma_1$ state has grown further and is becoming comparable to that in the $A\,^1\Pi_1$ state. There is now also a small amplitude of the wave packet in the $a\,^3\Pi_1$ state. At 14.5 fs the amplitude of the wave packet in the $a\,^3\Pi_1$ state has grown considerably and

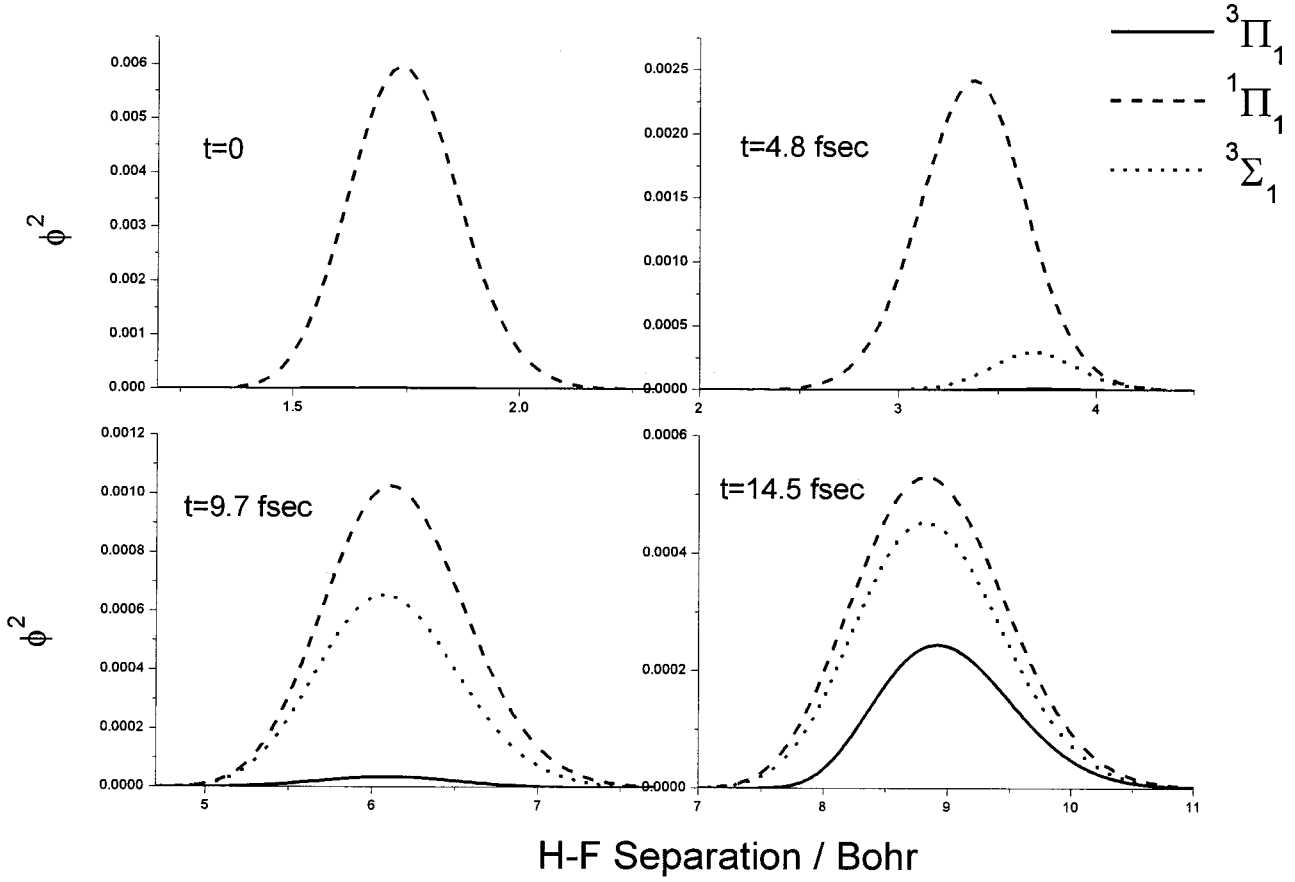

FIG. 1. Square of wave packets in the $a\ ^3\Pi_1$ (solid line), $A\ ^1\Pi_1$ (dashed line), and $1\ ^3\Sigma_1^+$ (dotted line) adiabatic excited electronic states of HF at different times.

the amplitude in the $1\ ^3\Sigma_1$ state has also increased. The whole of the photodissociation dynamics takes about 20 fs.

The photofragmentation **T** matrix elements, $\langle \Psi^-_{n,\Omega} | \hat{\mathbf{d}}_q | \Psi_{\Omega_i} \rangle$, are computed from the wave packets in the different adiabatic electronic states using Eq. (11). The dynamical functions are then computed using Eq. (6) and these are used to compute the anisotropy parameters using the equations of Appendix B. Figure 2 shows the anisotropy parameters with $\tilde{Q}=0$, $\mathbf{a}_0^{(K)}(\perp)$, for the photodissociation of HF($v=0$). The notation $\perp$, introduced by Rakitzis and Zare,[9] indicates that the transition involved is a perpendicular transition. The computed absorption cross section for the photodissociation of HF($v=0$)[14] has a Gaussian type line shape with a maximum at 83 467 cm^{-1} and a half-width of 12 457 cm^{-1}. This results in a cross section which has significant values when depicted graphically over the energy range 70 000 to 100 000 cm^{-1}. From the figure we see that all the $\tilde{Q}=0$ anisotropy parameters have significant values but remain relatively constant over the energy range 77 500 to 90 000 cm^{-1} which includes the main peak of the absorption cross section. At lower photon energies the parameters decrease significantly. Our analysis below will show that the values of these parameters are directly related to the probabilities of electronically nonadiabatic transitions between the three adiabatic electronic states involved. In the absence of any electronically nonadiabatic transitions for instance the anisotropy parameter $\mathbf{a}_0^{(1)}(\perp)$ is predicted to have a value of 0.7746. At the peak of the absorption spectrum $\mathbf{a}_0^{(1)}(\perp)$ has a value of 0.5973. The difference between these two values is a direct quantitative measure of the presence of electronically nonadiabatic transitions which are also clearly demonstrated in Fig. 1.

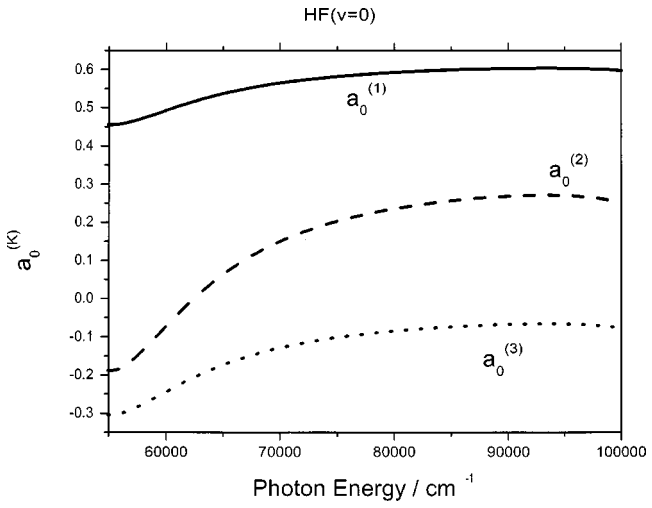

FIG. 2. Anisotropy parameters $\mathbf{a}_0^{(K)}(\perp)$ as a function of photon energy for photodissociation of HF initially in its ground, $v=0$, vibrational state.

Figure 3 shows the anisotropy parameters with $\tilde{Q}=2$,

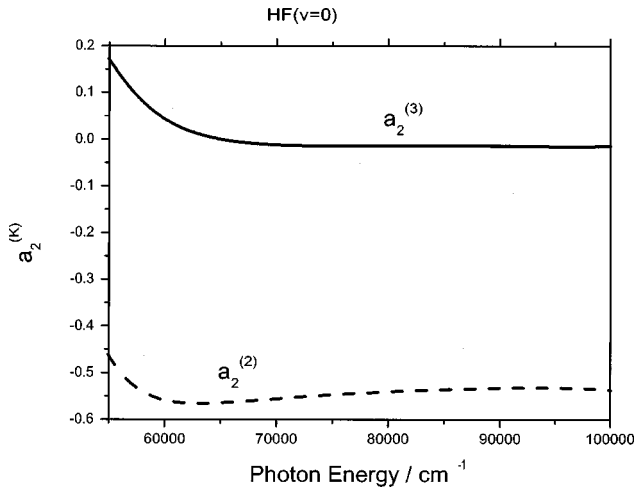

FIG. 3. Anisotropy parameters $\mathbf{a}_2^{(K)}(\perp)$ as a function of photon energy for photodissociation of HF initially in its ground, $v=0$, vibrational state.

$\mathbf{a}_2^{(K)}(\perp)$, for the photodissociation of HF($v=0$). These parameters are again relatively constant over the energy range where the absorption cross section has its peak. At lower energies, they show a small dip and then rise significantly as the energy decreases further. Our analysis in Sec. IV B will show that these parameters carry information concerning both the probability of electronically nonadiabatic transitions and the relative phases ($\Delta\phi$) of the photofragmentation **T** matrix elements associated with the $A\,^1\Pi_1$ and the $a\,^3\Pi_1$ states. The anisotropy parameter $\mathbf{a}_2^{(3)}(\perp)$ will be shown to be proportional to $\sin\Delta\phi$ and is close to zero as $\Delta\phi$ is close to zero. The anisotropy parameter $\mathbf{a}_2^{(2)}(\perp)$ will be shown on the other hand to be proportional to $\cos\Delta\phi$ and this parameter is distinctly nonzero as a result of the substantial probability of electronically nonadiabatic transitions.

B. Interpretation of anisotropy parameters

The consequences of the dynamics of the photodissociation process are entirely contained in the photofragmentation **T** matrix elements.[14] Equation (6) and Appendix B show that the **T** matrix elements are central to the calculation of the anisotropy parameters. Let us denote the **T** matrix elements corresponding to dissociation via the $a\,^3\Pi_1$, $A\,^1\Pi_1$, and $1\,^3\Sigma_1^+$ excited electronic states by

$$\langle\Psi_{n,1}^-|\hat{\mathbf{d}}_q|\Psi_0\rangle = r_n e^{i\phi_n}, \tag{13}$$

where the index n stands for $n=\alpha$ ($a\,^3\Pi_1$), β ($A\,^1\Pi_1$), and γ ($1\,^3\Sigma_1^+$).

The value r_n in Eq. (13) is the modulus of the corresponding photofragmentation **T** matrix. In the case of HF photodissociation, where only the $A\,^1\Pi_1$ molecular state can be optically excited from the ground electronic state, the values r_n are directly related to the probabilities of nonadiabatic transitions between the state $A\,^1\Pi_1$ and two other states involved,

$$\begin{aligned} r_\alpha^2 &= p_1, \\ r_\beta^2 &= 1-p_1-p_2, \\ r_\gamma^2 &= p_2. \end{aligned} \tag{14}$$

The probability p_2 is the branching fraction for producing the excited F($^2P_{1/2}$) state. It is calculated from the partial cross section for producing the F($^2P_{1/2}$) state divided by the total absorption cross section. The probability p_1 is the probability of nonadiabatic transitions from the $A\,^1\Pi_1$ to the $a\,^3\Pi_1$ state.

Using the definition above for the photofragmentation **T** matrix elements, Eq. (13), Eq. (6) for the dynamical functions and the values given in Table I for the matrix elements $\mathcal{T}^{n\Omega}_{j_A\Omega_A j_B\Omega_B}$, we obtain the following expressions for the diagonal elements of the dynamical functions, $f_K(1,1)$, for the detection of ground state $^2P_{3/2}$ fluorine photofragments:

$$f_0(1,1) = \tfrac{1}{2}(1-p_2), \tag{15}$$

$$f_1(1,1) = \frac{1}{2\sqrt{15}}(3-2p_1-3p_2), \tag{16}$$

$$f_2(1,1) = \frac{1}{2\sqrt{5}}(1-2p_1-p_2), \tag{17}$$

$$f_3(1,1) = \frac{1}{2\sqrt{35}}(1-4p_1-p_2). \tag{18}$$

Inserting these expressions into the equations given in Appendix B results in the following expressions for the $\tilde{Q}=0$ anisotropy parameters, $\mathbf{a}_0^{(K)}(\perp)$:

$$\mathbf{a}_0^{(1)}(\perp) = \frac{3-2p}{\sqrt{15}}, \tag{19}$$

$$\mathbf{a}_0^{(2)}(\perp) = \frac{4(1-2p)}{5}, \tag{20}$$

$$\mathbf{a}_0^{(3)}(\perp) = \frac{4(1-4p)}{5\sqrt{15}}, \tag{21}$$

where

$$p = \frac{p_1}{1-p_2}. \tag{22}$$

Similarly, if we define the phase difference between the photofragmentation **T** matrix elements for the $a\,^3\Pi_1$ and the $A\,^1\Pi_1$ states as $\Delta\phi=\phi_\alpha-\phi_\beta$, we can derive the following expressions for the nondiagonal dynamical functions:

$$f_0(1,-1) = f_1(1,-1) = 0, \tag{23}$$

$$f_2(1,-1) = \frac{\sqrt{2}}{\sqrt{5}}\sqrt{(1-p_1-p_2)p_1}\cos\Delta\phi, \tag{24}$$

$$f_3(1,-1) = -i\frac{\sqrt{2}}{\sqrt{7}}\sqrt{(1-p_1-p_2)p_1}\sin\Delta\phi. \tag{25}$$

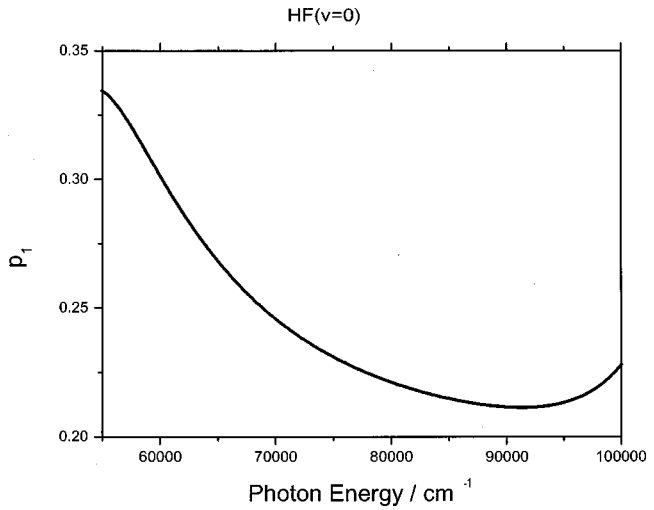

FIG. 4. Transition probability, p_1, from $A\,^1\Pi_1$ to $a\,^3\Pi_1$ adiabatic electronic state as a function of photon energy for the photodissociation process $\mathrm{HF}(v=0)+h\nu\rightarrow\mathrm{H}+\mathrm{F}$. See text for details.

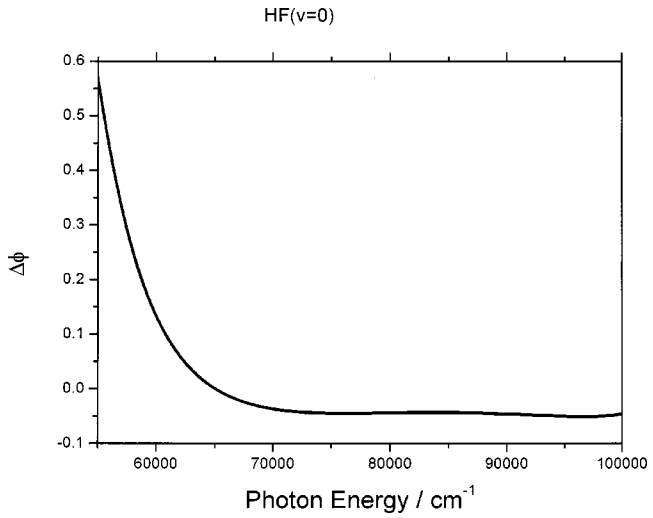

FIG. 6. Phase difference, $\Delta\phi$, between photofragmentation **T** matrix elements for the $A\,^1\Pi_1$ and $a\,^3\Pi_1$ adiabatic electronic states as a function of energy for the photodissociation process $\mathrm{HF}(v=0)+h\nu\rightarrow\mathrm{H}+\mathrm{F}$. See text for details.

From these we can derive expressions for the $\tilde{Q}=2$ anisotropy parameters, $\mathbf{a}_2^{(K)}(\perp)$,

$$\mathbf{a}_2^{(2)}(\perp)=-\frac{4\sqrt{2}}{25}\sqrt{(1-p)p}\cos\Delta\phi, \tag{26}$$

$$\mathbf{a}_2^{(3)}(\perp)=\frac{4\sqrt{2}}{5\sqrt{3}}\sqrt{(1-p)p}\sin\Delta\phi. \tag{27}$$

The anisotropy parameters in Eqs. (19)–(21) and in Eqs. (26) and (27) depend only on three key dynamical parameters; p_2 (or alternatively p), p_1, and $\Delta\phi$. These key dynamical parameters can all, in principle, be derived from experimentally measurable quantities; the branching fraction and the anisotropy parameters. We have presented *ab initio* calculated values of the anisotropy parameters in Figs. 2 and 3 and the computed branching fraction has been presented in Ref. 14. We have used the computed branching fraction to calculate p_2 as a function of energy. Once we have p_2 we can compute p_1 from $\mathbf{a}_0^{(1)}(\perp)$, see Eqs. (19) and (22). In a similar way we could compute the probability p_1 using either $\mathbf{a}_0^{(2)}(\perp)$ [see Eq. (20)], together with Eq. (22) or $\mathbf{a}_0^{(3)}(\perp)$ [see Eq. (21)], again in conjunction with Eq. (22). Thus once we have extracted p_2, either from experimental measurements or from the computed results, the values of p_1 can be derived from any one of the three $\tilde{Q}=0$ anisotropy parameters (see Fig. 2). There are, therefore, three different ways in which we can deduce the values of p_1 from experimental results, or as we will do here, compute them from the *ab initio* calculated values.

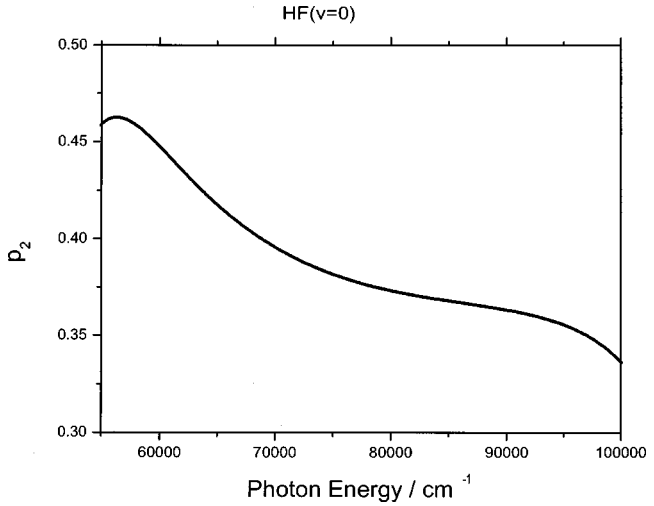

FIG. 5. Branching fraction, p_2, for the production of $\mathrm{F}(^2P_{1/2})$ as a function of photon energy in the photodissociation process $\mathrm{HF}(v=0)+h\nu\rightarrow\mathrm{H}+\mathrm{F}$. See text for details.

Figures 4 and 5 show the values of p_1 and p_2, respectively, calculated in this way. The values of p_1, shown in Fig. 4, have been computed in all three ways discussed above. All three calculations give identical results. This confirms that our dynamical model is at least internally consistent. The ''statistical'' limit for this transition probability is 0.5. The figure therefore shows that the dynamics do not result in a statistical distribution. The probability for this transition varies considerably with energy and is consistent with the magnitudes of the $A\,^1\Pi_1$ and $a\,^3\Pi_1$ wave packets shown in Fig. 1.

The $\tilde{Q}=2$ anisotropy parameters, see Fig. 3, can be used to calculate the phase difference, $\Delta\phi$ [see Eqs. (26) and (27)]. Again the two equations provide two independent ways of deducing the values of $\Delta\phi$. Figure 6 shows the phase difference calculated from the anisotropy parameters. Just as in the case of p_1, the values of $\Delta\phi$ calculated from $\mathbf{a}_2^{(2)}(\perp)$ and from $\mathbf{a}_2^{(3)}(\perp)$ are identical, again confirming the validity of the paramatrization used in Eqs. (13)–(27). The phase difference is very small, negative, and nearly constant over the entire significant energy range, i.e., over the range 70 000 to 100 000 cm^{-1}. At lower energies, at which the absorption cross section is negligibly small, the phase difference increases sharply with decreasing photon energy. The small value of the phase difference over the photon energy

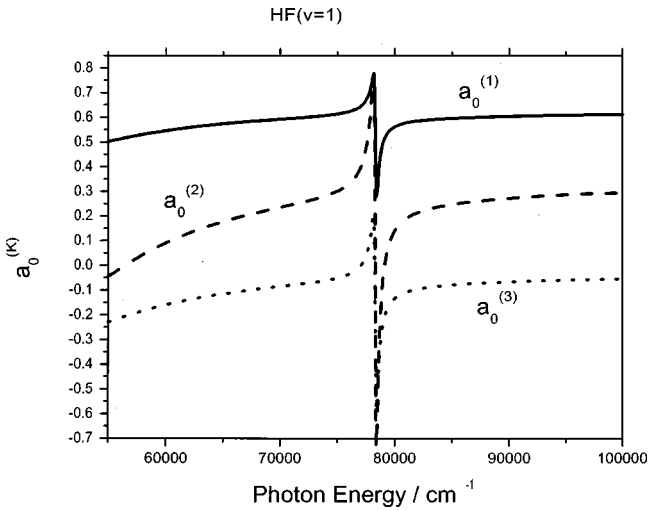

FIG. 7. Anisotropy parameters $\mathbf{a}_0^{(K)}(\perp)$ as a function of photon energy for photodissociation of HF initially in its first excited, $v=1$, vibrational state.

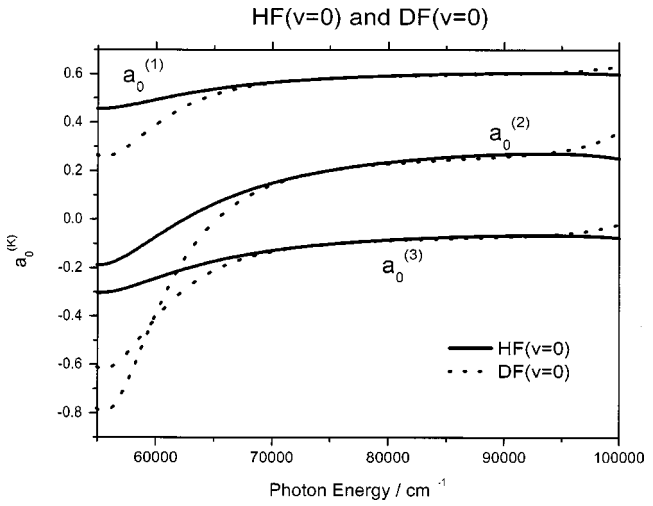

FIG. 9. Anisotropy parameters $\mathbf{a}_0^{(K)}(\perp)$ as a function of photon energy for photodissociation of HF (solid line) and DF (dotted line) initially in their ground, $v=0$, vibrational states.

range 70 000 to 100 000 cm^{-1} is consistent with Fig. 1. This shows that the amplitude in the $a\,^3\Pi_1$ state builds up during the very final part of the breakup processes. Thus the amplitude of the wave packet remains in the $A\,^1\Pi_1$ state until near the end of the breakup when a portion of it is transferred through electronically nonadiabatic transitions to the $a\,^3\Pi_1$ state. This accounts for the fact that the phase of the wave packet in the two states is nearly identical in the asymptotic region.

C. Anisotropy parameters arising from the photodissociation of HF($v=1$)

Figures 7 and 8 show the anisotropy parameters for $\tilde{Q}=0$ and $\tilde{Q}=2$, respectively, for the photodissociation process $\mathrm{HF}(v=1)+h\nu\rightarrow\mathrm{H}+\mathrm{F}$. All the anisotropy parameters display a sharp change around a photon energy of 78 269 cm^{-1}. A similar sharp change was observed in the branching fractions reported in Ref. 14. The origin of this change is the node in the HF($v=1$) vibrational wave function and the resulting near-zero values of the partial cross sections close to this photon energy. The nonzero values of $\mathbf{a}_0^{(K)}(\perp)$ and of $\mathbf{a}_2^{(2)}(\perp)$ again confirm that electronically nonadiabatic transitions play an important part in the breakup dynamics. We have calculated the electronically nonadiabatic transition probabilities, p_1 and p_2, and the phase difference, $\Delta\phi$, for the photodissociation of HF($v=1$). These again all fit the model proposed in Eqs. (13)–(27).

D. Anisotropy parameters arising from the photodissociation of DF

Figures 9 and 10 show the computed $\mathbf{a}_0^{(K)}(\perp)$ and $\mathbf{a}_2^{(K)}(\perp)$ anisotropy parameters, respectively, arising from the photodissociation of DF($v=0$). The anisotropy parameters for DF are shown as dotted lines. The parameters for HF are shown as solid lines in the figures for comparison. The main conclusion to be drawn from the figures is that the anisotropy

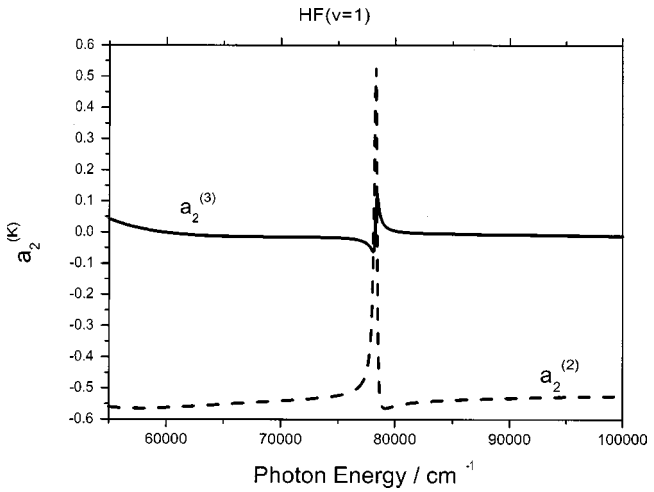

FIG. 8. Anisotropy parameters $\mathbf{a}_2^{(K)}(\perp)$ as a function of photon energy for photodissociation of HF initially in its first excited, $v=1$, vibrational state.

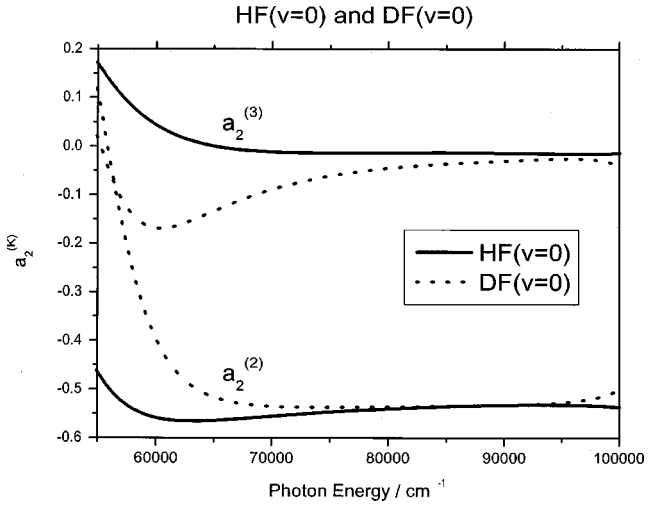

FIG. 10. Anisotropy parameters $\mathbf{a}_2^{(K)}(\perp)$ as a function of photon energy for photodissociation of HF (solid line) and DF (dotted line) initially in their ground, $v=0$, vibrational states.

parameters for the photodissociation of DF are surprisingly similar to those of HF. If we remember that the photon energy range over which the HF absorption cross section has a significant magnitude is 70 000 to 100 000 cm^{-1}, then we see that over this energy range the $\mathbf{a}_0^{(K)}(\perp)$ anisotropy parameters are almost identical (see Fig. 9). The $\mathbf{a}_2^{(K)}(\perp)$ anisotropy parameters for DF, Fig. 10, differ more from their HF counterparts than do the $\mathbf{a}_0^{(K)}(\perp)$ parameters. From Eqs. (26) and (27) we see that these parameters are dependent on the phase difference between the photofragmentation **T** matrix elements for the $A\,^1\Pi_1$ to $a\,^3\Pi_1$ adiabatic electronic states. This phase difference is affected by the isotope change from HF to DF more than are the nonadiabatic transition probabilities p_1 and p_2.

V. CONCLUSIONS

The paper presents the first *ab initio* calculation of photofragmentation anisotropy parameters. The analysis of these parameters given in the paper shows how it would be possible, for the simple case considered here, to extract electronically nonadiabatic transition probabilities and the phase difference between photofragmentation **T** matrix elements from experimental measurements. We have used our calculated results (Figs. 2 and 3), in the place of experimentally measured data, to illustrate how these fundamental molecular dynamical quantities may be extracted from observable data. Our results show clearly that electronically nonadiabatic transition probabilities play an important role in the breakup dynamics, see Figs. 4 and 5. In this particular case our results also show that the phase difference between photofragmentation **T** matrix elements for breakup in the two different adiabatic states which lead to ground state photofragments, $H(^2S_{1/2})$ and $F(^2P_{3/2})$, is very small over most of the photon energy range in which the absorption cross section has a significant nonzero value. Our analysis of the wave packets corresponding to the different adiabatic electronic states (see Fig. 1) shows that the probable reason for this is that the wave packet flux remains on the $A\,^1\Pi_1$ state during nearly the entire breakup process and is transferred to the $a\,^3\Pi_1$ state only in the very final stage of the dissociation. The analysis also shows that a substantial fraction of the flux is transferred from the $A\,^1\Pi_1$ to the $1\,^3\Sigma_1^+$ state at a much earlier stage.

The anisotropy parameters for the photodissociation of vibrationally excited HF in its $v=1$ vibrational state show a sharp change in their value over a very narrow photon energy range (see Figs. 7 and 8). This change occurs at the same photon energy as a similar change in the branching fractions (see Ref. 14) and is due to a near zero in the partial absorption cross sections which in turn arises from the nodal structure of the initial vibrational wave function.

The anisotropy parameters for the photodissociation of DF are found to be very similar to those arising from the photodissociation of HF. The largest differences are found for the parameters describing the coherent production of the $\Omega=1$ and $\Omega=-1$ substates of the $F(^2P_{3/2})$ fragment in a body-fixed reference frame [i.e., $\mathbf{a}_2^{(2)}(\perp)$ and $\mathbf{a}_2^{(3)}(\perp)$]. These parameters depend on the phase difference between photofragmentation **T** matrix elements and we conclude that this phase difference is the dynamical quantity most strongly affected by the change of isotope from H to D.

ACKNOWLEDGMENTS

We thank E. R. Wouters for valuable discussions. We thank the Royal Society for funding part of the collaboration which permitted this research. We also acknowledge funding from collaborative grant INTAS Ref. N 31573 for funding this work.

APPENDIX A: STATE MULTIPOLES AND DYNAMICAL FACTORS

Equations (5) and (6) can be derived from the general expressions for the photodissociation cross sections $\sigma^{j_A}_{m'_A;m_A}(\theta,\phi)$, Eqs. (1) and (2), by a sequence of transformations and manipulations. The derivation of the cross sections has been discussed in detail in Ref. 18, and a closely related discussion has been given in Ref. 15. We will not repeat this long and involved derivation here, but will refer the reader to these papers and will discuss only some new points raised by the present work.

The cross section in Eq. (2) is expressed in terms of the asymptotic fragment energy eigenfunctions $|j_A m_A\rangle$ and $|j_B m_B\rangle$, while the "n" subscripts and superscripts in Eq. (6) [i.e., in $\Psi^-_{n,\Omega}(R,\mathbf{r},E)$ and $\mathcal{T}^{n\Omega}_{j_A\Omega_A j_B\Omega_B}$] refer to a set of *adiabatic* internal electron molecular states $\Psi^{\mathrm{el}}_{n,\Omega}(\mathbf{r},R)$ [see Eq. (4)] which are the orthonormal eigenstates of the full Hamiltonian, $H_{\mathrm{int}}(\mathbf{r})+V(\mathbf{r},R)$, for fixed values of R. The index n is a dissociation channel number and the Hamiltonian $H_{\mathrm{int}}(\mathbf{r})$ refers to the sum of the noninteracting Hamiltonians of the fragments.

Three transformations are needed to relate the two different sets of fragment states to each other. First we must transform from the "$|j_A m_A\rangle|j_B m_B\rangle$" basis to the basis of the total angular momentum of the fragments $\mathbf{j}=\mathbf{j_A}+\mathbf{j_B}$ and its space-fixed z component $m=m_A+m_B$. This transformation is given by

$$|jm\rangle=\sum_{m_A m_B} C^{jm}_{j_A m_A j_B m_B}|j_A m_A\rangle|j_B m_B\rangle, \tag{A1}$$

where $C^{jm}_{j_A m_A j_B m_B}$ is a Clebsch–Gordan coefficient.

The scattering equations for the dissociation of the molecule are most conveniently solved in a body-fixed coordinate system, in which the z axis is the interfragment separation vector, **R**. We must now transform the functions $|jm\rangle$ from the space-fixed to the body-fixed reference frame. This transformation is[15,18]

$$|j\Omega\rangle=\sum_m D^j_{\Omega m}{}^*(\phi,\theta,0)|jm\rangle. \tag{A2}$$

The functions, $|j\Omega\rangle$ are *diabatic* functions in the sense that they are built up from the energy eigenfunctions of the separated fragments and do not change with interfragment distance, R. To relate these to the *adiabatic* internal electron

molecular states $\Psi^{\rm el}_{n,\Omega}(\mathbf{r},R)$ we require a further transformation. In the asymptotic region the function $\Psi^{\rm el}_{n,\Omega}(\mathbf{r},R)$ can be written in the form

$$\Psi^{\rm el}_{n,\Omega}(\mathbf{r},R) \overset{R\to\infty}{\sim} \sum_j \langle j\Omega|n\Omega\rangle|j\Omega\rangle. \tag{A3}$$

We can now use the relationship in the body-fixed coordinate system

$$|j_A\Omega_A\rangle|j_B\Omega_B\rangle = \sum_j C^{j\Omega}_{j_A\Omega_A j_B\Omega_B}|j\Omega\rangle. \tag{A4}$$

Combining Eqs. (4) and (A4) and comparing with Eq. (A3), we can derive a relationship for the $\langle j\Omega|n\Omega\rangle$ coefficients in Eq. (A3) in terms of the matrices $\mathcal{T}^{n\Omega}_{j_A\Omega_A j_B\Omega_B}$ in Eq. (4),

$$\langle j\Omega|n\Omega\rangle = \sum_{\Omega_A\Omega_B} C^{j\Omega}_{j_A\Omega_A j_B\Omega_B}\mathcal{T}^{n\Omega}_{j_A\Omega_A j_B\Omega_B}. \tag{A5}$$

Inversion of (A3) gives

$$|j\Omega\rangle \overset{R\to\infty}{\sim} \sum_n \langle n\Omega|j\Omega\rangle\Psi^{\rm el}_{n,\Omega}(\mathbf{r},R). \tag{A6}$$

Inverting Eqs. (A1) and (A2) now yields a relationship between the adiabatic body-fixed coordinate fragment eigenfunctions $\Psi^{\rm el}_{n,\Omega}(\mathbf{r},R)$ and the space-fixed diabatic eigenstates $|j_Am_A\rangle|j_Bm_B\rangle$,

$$|j_Am_A\rangle|j_Bm_B\rangle \overset{R\to\infty}{\sim} \sum_{jm} C^{jm}_{j_Am_Aj_Bm_B}\sum_\Omega D^j_{\Omega m}(\phi,\theta,0) \times\sum_n \langle n\Omega|j\Omega\rangle\Psi^{\rm el}_{n,\Omega}(\mathbf{r},R). \tag{A7}$$

These transformations, combined with the equations in Ref. 18, enable us to derive Eqs. (5) and (6) in the main body of the paper.

APPENDIX B: ORIENTATION AND ALIGNMENT ANISOTROPY PARAMETERS

The rank K of the dynamical functions $f_K(q,q')$, Eq. (6), describing the magnetic sublevel populations of the ground state fluorine fragment F($^2P_{3/2}$) is limited to $K=0,1,2,3$. Only the following two combinations of the indices q,q': $q=1$, $q'=1$; $q=1$, $q'-1$ should be considered in Eq. (6) because of the absence of parallel transitions in the HF molecule ($\beta=-1$) and due to the symmetry rules, see Eq. (7). The corresponding rank $K=1,2,3$ molecular frame ($\mathbf{a}^{(K)}_Q$) and laboratory frame (α_K,η_K,s_K) anisotropy parameters in terms of the dynamical functions are given below. For generality the relationships between the molecular frame and laboratory frame anisotropy parameters are given for an arbitrary value of the β parameter.

(1) Rank $K=1$ anisotropy parameters,

$$\mathbf{a}^{(1)}_0(\perp) = \frac{f_1(1,1)}{f_0(1,1)}, \quad \frac{2-\beta}{6}\mathbf{a}^{(1)}_0(\perp) = \alpha_1. \tag{B1}$$

(2) Rank $K=2$ anisotropy parameters,

$$\begin{aligned}
&\mathbf{a}^{(2)}_0(\perp) = V_2(j_A)^{-1}\frac{f_2(1,1)}{f_0(1,1)},\\
&\frac{2-\beta}{10}\mathbf{a}^{(2)}_0(\perp) = \alpha_2 + s_2,\\
&\mathbf{a}^{(2)}_2(\perp) = -\frac{1}{2}V_2(j_A)^{-1}\frac{f_2(1,-1)}{f_0(1,1)},\\
&-\frac{2(2-\beta)}{5\sqrt{6}}\mathbf{a}^{(2)}_2(\perp) = \eta_2,
\end{aligned} \tag{B2}$$

where

$$V_2(j) = \left[\frac{j(j+1)}{(2j+3)(2j-1)}\right]^{1/2}.$$

(3) Rank $K=3$ anisotropy parameters,

$$\begin{aligned}
&\mathbf{a}^{(3)}_0(\perp) = V_3(j_A)^{-1}\frac{f_3(1,1)}{f_0(1,1)}, \quad \frac{2-\beta}{6}\mathbf{a}^{(3)}_0(\perp) = \alpha_3,\\
&\mathbf{a}^{(3)}_2(\perp) = \frac{i}{2}V_3(j_A)^{-1}\frac{f_3(1,-1)}{f_0(1,1)},\\
&\frac{\sqrt{5}(2-\beta)}{6}\mathbf{a}^{(3)}_2(\perp) = \eta_3,
\end{aligned} \tag{B3}$$

where

$$V_3(j) = \frac{j(j+1)}{[(j-1)(j+2)(2j-1)(2j+3)]^{1/2}}.$$

[1] Y. Mo, H. Katayanagi, M. C. Heaven, and M. C. Suzuki, Phys. Rev. Lett. **77**, 830 (1996).
[2] A. T. J. B. Eppink, D. H. Parker, M. H. M. Janssen, B. Buijsse, and W. J. van der Zande, J. Chem. Phys. **108**, 1305 (1998).
[3] Y. Wang, H. P. Loock, J. Cao, and C. X. W. Qian, J. Chem. Phys. **102**, 808 (1995).
[4] M. L. Costen, S. W. North, and G. E. Hall, J. Chem. Phys. **111**, 6735 (1999).
[5] T. P. Rakitzis, S. A. Kandel, A. J. Alexander, Z. H. Kim, and R. N. Zare, Science **281**, 1346 (1998).
[6] A. S. Bracker, E. R. Wouters, A. G. Suits, Y. T. Lee, and O. S. Vasyutinskii, Phys. Rev. Lett. **80**, 1626 (1998).
[7] R. N. Dixon, J. Chem. Phys. **85**, 1866 (1986).
[8] C. H. Greene and R. N. Zare, Annu. Rev. Phys. Chem. **33**, 119 (1982).
[9] T. P. Rakitzis and R. N. Zare, J. Chem. Phys. **110**, 3341 (1999).
[10] T. P. Rakitzis, G. E. Hall, M. L. Costen, and R. N. Zare, J. Chem. Phys. **111**, 8751 (1999).
[11] A. S. Bracker, E. R. Wouters, A. G. Suits, and O. S. Vasyutinskii, J. Chem. Phys. **110**, 6749 (1999).
[12] E. R. Wouters, M. Ahmed, D. S. Peterska, A. S. Bracker, A. G. Suits, and O. S. Vasyutinskii, "Imaging the Atomic Orientation and Alignment in Photodissociation," in *Imaging in Chemical Dynamics*, edited by A. G. Suits and R. E. Continetti (American Chemical Society, Washington DC, 2000), p. 238.
[13] Y. Asano and S. Yabushita, J. Phys. Chem. A **105**, 9873 (2001).
[14] A. Brown and G. G. Balint-Kurti, J. Chem. Phys. **113**, 1870 (2000); **113**, 1879 (2000).
[15] G. G. Balint-Kurti and M. Shapiro, Chem. Phys. **61**, 137 (1981).
[16] M. S. Child, *Molecular Collision Theory* (Dover, Mineola, New York, 1996).
[17] G. G. Balint-Kurti and M. Shapiro, "Quantum Theory of Molecular Photodissociation," in *Photodissociation and Photoionization*, edited by K. P. Lawley (Wiley, New York, 1985), p. 403.
[18] G. G. Balint-Kurti, L. Füsti-Molnár, and A. Brown, Phys. Chem. Chem. Phys. **3**, 702 (2001).

[19] L. D. A. Siebbeles, M. Glass-Maujean, O. S. Vasyutinskii, J. A. Beswick, and O. Roncero, J. Chem. Phys. **100**, 3610 (1994).
[20] K. Blum, *Density Matrix Theory and Applications*, 2nd ed. (Plenum, New York, 1996).
[21] R. N. Zare, *Angular Momentum* (World Scientific, New York, 1988).
[22] W. Happer, Rev. Mod. Phys. **44**, 169 (1972).
[23] E. E. Nikitin and S. Ya. Umanskii, *Theory of Slow Atomic Collisions* (Springer, Berlin, 1984).
[24] O. S. Vasyutinskii, Sov. Phys. JETP **54**, 855 (1981).
[25] D. V. Kupriayanov and O. S. Vasyutinskii, Chem. Phys. **171**, 25 (1993).
[26] J. A. Beswick and O. S. Vasyutinskii, Comments At. Mol. Phys. **42**, 69 (1998).
[27] D. A. Varshalovich, A. N. Moskalev, and V. K. Khersonskii, *Quantum Theory of Angular Momentum* (World Scientific, Singapore, 1988).
[28] E. B. Alexandrov, M. P. Chaika, and G. I. Khvostenko, *Interference of Atomic States* (Springer, Berlin, 1993).
[29] T. P. Rakitzis, P. C. Samartzis, and T. N. Kitsopoulos, Phys. Rev. Lett. **87**, 123001 (2001).
[30] A. R. Edmonds, *Angular Momentum in Quantum Mechanics* (Princeton University Press, Princeton, NJ, 1960).
[31] B. V. Picheyev, A. G. Smolin, and O. S. Vasyutinskii, J. Phys. Chem. **101**, 7614 (1997).
[32] A. J. Alexander, Z. H. Kim, S. A. Kandel, R. N. Zare, Y. Asano, and S. Yabushita, J. Chem. Phys. **113**, 9022 (2000).
[33] G. G. Balint-Kurti, R. N. Dixon, and C. C. Marston, J. Chem. Soc., Faraday Trans. **86**, 1741 (1990); note that the right-hand side of Eqs. (3) and (24) should be multiplied by a factor of 4π.
[34] G. G. Balint-Kurti, R. N. Dixon, and C. C. Marston, Int. Rev. Phys. Chem. **11**, 317 (1992).
[35] D. V. Kupriayanov, B. N. Sevastianov, and O. S. Vasyutinskii, Z. Phys. D: At. Mol. Clusters **15**, 105 (1990).
[36] MOLPRO is a package of *ab initio* programs written by H.-J. Werner and P. J. Knowles, with contributions from R. D. Amos, A. Bernhardsson, A. Berning *et al.*
[37] R. A. Kendall, T. H. Dunning, Jr., and R. J. Harrison, J. Chem. Phys. **96**, 6796 (1992); D. E. Woon and T. H. Dunning, Jr., *ibid.* **98**, 1358 (1993).
[38] P. M. Regan, D. Ascenzi, A. Brown, G. G. Balint-Kurti, and A. J. Orr-Ewing, J. Chem. Phys. **112**, 10259 (2000).